Thermal Transitions in Human Very-Low-Density Lipoprotein: Fusion, Rupture, and Dissociation of HDL-like Particles†

Madhumita Guha, Cheryl England, Haya Herscovitz, and Olga Gursky*

Department of Physiology and Biophysics, Boston University School of Medicine, Boston, Massachusetts 02118

Received January 24, 2007; Revised Manuscript Received March 15, 2007

ABSTRACT: Very-low-density lipoproteins (VLDL) are metabolic precursors of low-density lipoproteins (LDL) and a risk factor for atherosclerosis. Human VLDL are heterogeneous complexes containing a triacylglycerol-rich apolar lipid core and polar surface composed of phospholipids, a nonexchangeable apolipoprotein B, and exchangeable apolipoproteins E and Cs. We report the first stability study of VLDL. Circular dichroism and turbidity data reveal an irreversible heat-induced VLDL transition that involves formation of larger particles and repacking of apolar lipids but no global protein unfolding. Heating rate effect on the melting temperature indicates a kinetically controlled reaction with high activation energy, E_a. Arrhenius analysis of the turbidity data reveals two kinetic phases with $E_a = 53 \pm 7$ kcal/mol that correspond to distinct morphological transitions observed by electron microscopy. One transition involves VLDL fusion, partial rupture, and dissociation of small spherical particles ($d = 7-15$ nm), and another involves complete lipoprotein disintegration and lipid coalescence into droplets accompanied by dissociation of apolipoprotein B. The small particles, which are unique to VLDL denaturation, are comparable in size and density to high-density lipoproteins (HDL); they have an apolar lipid core and polar surface composed of exchangeable apolipoproteins (E and possibly Cs) and phospholipids. We conclude that, similar to HDL and LDL, VLDL are stabilized by kinetic barriers that prevent particle fusion and rupture and decelerate spontaneous interconversion among lipoprotein classes and subclasses. In addition to fusion, VLDL disruption involves transient formation of HDL-like particles that may mimic protein exchange among VLDL and HDL pools in plasma.

Plasma lipoproteins, including high-, low-, intermediate-, and very-low-density lipoproteins (HDL,[1] LDL, IDL, and VLDL), are macromolecular complexes of lipids and proteins (termed apolipoproteins) that mediate lipid transport and metabolism and are central in the development of coronary artery disease. HDL are antiatherogenic, LDL are proatherogenic, and VLDL are not only direct metabolic precursors of LDL but also an independent risk factor for atherosclerosis (*1*−*8*). VLDL are the major carriers of triacylglycerols (TG) in plasma. Human VLDL form heterogeneous populations of spherical particles that contain an apolar core composed mainly of TG and cholesterol esters (CE) and polar surface composed of a cholesterol-containing phospholipid monolayer and proteins. The proteins include one copy of nonexchangeable apolipoprotein B (apoB, 550 kDa) and multiple copies of exchangeable apolipoproteins, mainly apoE (34 kDa) and apoCs (6−9 kDa), that comprise over 50% of the total VLDL protein content. Metabolic remodeling by lipolytic enzymes converts VLDL into LDL that contain apoB as their sole protein, while the dissociated apoE and apoCs enter the HDL pool (*2*, *4*). Structural and stability properties of HDL and LDL have been intensely investigated by spectroscopic and calorimetric methods (refs *9*−*11* and references therein), yet structural studies of VLDL have been limited to nondenaturing conditions (*12*−*14*). Here we report the first stability study of human VLDL.

Our recent thermal and chemical denaturation analyses have shown that HDL and LDL are stabilized by kinetic barriers, and have revealed distinct kinetic steps in the disruption of these lipoproteins (*9*−*11*). The first step involves partial protein dissociation and lipoprotein fusion that compensates for the particle surface depletion of the protein moiety; the next step involves additional protein dissociation leading to lipoprotein rupture and release of the apolar core. These results prompted us to propose that kinetic barriers associated with particle fusion and rupture provide a universal natural strategy for lipoprotein stabilization and are important modulators of lipoprotein metabolism (*9*−*11*).

Now we test the hypothesis that, similar to HDL and LDL, the structural stability of VLDL is determined by kinetic barriers. However, vast differences in size and composition of HDL (that range in diameter from $d \sim 7-15$ nm and contain only exchangeable proteins), LDL ($d \sim 22$ nm, contain only nonexchangeable apoB), and VLDL ($d = 40-100$ nm, contain both exchangeable and nonexchangeable

† This work was supported by the National Institutes of Health Grants GM067260 and HL026355.

* Corresponding author. Mailing address: Department of Physiology and Biophysics, Boston University School of Medicine, W329, 715 Albany Street, Boston, MA 02118. Tel: (617) 638-7894. Fax: (617) 638-4041. E-mail: gursky@bu.edu.

[1] Abbreviations used: VLDL, very-low-density lipoprotein; LDL, low-density lipoprotein; HDL, high-density lipoprotein; apoB, apolipoprotein B; apoE, apolipoprotein E; apoCs, apolipoproteins C-I, C-II, and C-III; TG, triacylglyceride; CE, cholesterol ester; CD, circular dichroism; T-jump, temperature jump; EM, electron microscopy; SDS, sodium dodecyl sulfate; PAGE, polyacrylamide gel electrophoresis; TLC, thin-layer chromatography.

10.1021/bi7001532 CCC: $37.00
Published on Web 05/01/2007

proteins) are expected to result in distinctly different morphological transitions in these lipoproteins. In fact, clear differences were observed in the denaturation pathways of HDL and LDL. HDL denaturation involves formation of enlarged particles that are products of lipoprotein fusion and rupture and may mimic HDL fusion by plasma factors (*10*, *11*, *15*); in contrast, LDL denaturation involves not only formation of larger particles but also transient formation of smaller LDL-like particles that may resemble small dense LDL in plasma (*11*).

To test, for the first time, the heat-induced structural transitions in VLDL, we analyze thermal denaturation of VLDL from normolipidemic human plasma. The results establish the kinetic mechanism of VLDL stabilization and show that thermal denaturation of VLDL involves not only irreversible fusion and rupture but also transient formation of small spherical HDL-like particles. These particles may mimic the mode of protein and lipid exchange among HDL and VLDL pools in plasma.

MATERIALS AND METHODS

Sample Preparation. VLDL from six healthy volunteer donors were used. Single-donor VLDL were isolated from EDTA-treated plasma by density gradient ultracentrifugation in the density range 0.94−1.006 g/mL (*16*); total VLDL migrated as a single band on agarose gel. Total VLDL were ultracentrifuged for 30 min at 40 000 rpm, 4 °C and the clear fraction comprising mainly $VLDL_2$ subclass was collected and used to record the data shown in this work; similar data were recorded from total VLDL (not shown), suggesting that VLDL heterogeneity does not affect the key conclusions of this study. $VLDL_2$ stock solution of 1−2.5 mg/mL protein concentration (measured by modified Lowry assay (*17*)) was extensively dialyzed against the standard buffer used throughout this study (10 mM Na phosphate, 0.25 mM EDTA, 0.02% sodium azide, pH 7.6). The stock solution was stored in the dark at 4 °C and was used in 4 weeks, during which no protein degradation was detected by sodium dodecyl sulfate (SDS) polyacrylamide gradient gel electrophoresis (PAGE) and no changes in the protein secondary structure or lipoprotein stability were observed by circular dichroism (CD) and turbidity.

Circular Dichroism and Turbidity. CD and turbidity data were recorded using AVIV-215 or AVIV-62DS spectrometers with thermoelectric temperature control. Heat-induced turbidity changes were monitored by measuring dynode voltage, *V*, in CD experiments as described (*9*, *18*). CD spectra were recorded with 1 nm increment, 15−20 s/nm accumulation time from degassed VLDL solutions of 0.1−0.15 mg/mL protein concentrations using 0.5−2 mm path length closed cells for far-UV CD (185−250 nm) or of 0.5−0.6 mg/mL protein concentrations using 5 mm path length cell for near-UV/visible CD (250−500 nm). Far-UV CD data were normalized to protein concentration and expressed as molar residue ellipticity [Θ] that was calculated assuming the mean residue weight of 113. In the melting experiments, CD and turbidity data, Θ(*T*) and *V*(*T*), were recorded simultaneously at 220 or 320 nm during sample heating and consecutive cooling from 25 to 98 °C at a constant rate of 80 or 10 °C/h. No changes in the sample volume or protein concentration were detected after heating and cooling. In the kinetic temperature-jump (T-jump) experiments, the sample temperature was rapidly increased at $t = 0$ from 25 °C to a higher constant value, and the denaturation time course was monitored by CD and turbidity. Data analysis was carried out using an Arrhenius model as described (*9*). Briefly, kinetic data $V_{220}(t)$ recorded at each temperature were approximated by a multiexponential:

$$V_{220}(t) = A_1 \exp(-\tau_1/t) + A_2 \exp(-\tau_2/t) + ...$$

Here, A_1 and A_2 are the amplitudes of the kinetic phases, and τ_1 and τ_2 are the exponential relaxation times that are inverse of the reaction rates, $k = 1/\tau$. Since VLDL denaturation is irreversible, the reaction rate is equivalent to the denaturation rate. The relaxation times $\tau(T)$ were measured in T-jumps from 25 °C to several higher temperatures (75−95 °C), and the activation energy (enthalpy) E_a for each kinetic phase was determined from the slope of the corresponding Arrhenius plot, ln τ versus $1/T$.

Negative Staining Electron Microscopy. VLDL subjected to various thermal treatments were visualized at 25 °C by negative staining electron microscopy (EM) using a CM12 transmission electron microscope (Philips Electron Optics) as described (*9*, *10*). Particle size analysis was carried out in EXCEL using 300− 450 particles per image.

Biochemical Analysis of VLDL Denaturation Products. A VLDL sample was incubated at 83 °C and the aliquots taken after 0−120 min of incubation were analyzed by nondenaturing PAGE and Western blotting. Particle diameters assessed from nondenaturing PAGE (4−20%) were in good agreement with EM measurements.

For immunoblotting, the samples were subjected to nondenaturing PAGE, transferred to polyvinylidene fluoride membrane and probed with primary antibodies to apoE (Chemicon) and apoB using both monoclonal antibodies 1D1 (from Lipoprotein and Atherosclerosis Research Group, University of Ottawa Heart Institute) and polyclonal goat (Biodesign) and rabbit antibodies (custom-made by Sigma). The blots were probed with horseradish peroxidase-conjugated secondary antibodies (Sigma) and were visualized using an enhanced chemiluminescent system (Perkin-Elmer).

To analyze the composition of the small particles transiently formed at high temperatures, VLDL stock solution was incubated at 83 °C for 15 min and the bottom fraction containing mainly the small dense particles (as indicated by negative-staining EM) was isolated by 20−30 min centrifugation at 13 000 rpm (Biofuge, Thermo).

For protein analysis, the particles from this bottom fraction were delipidated by isopropanol and subjected to gradient SDS PAGE. For lipid analysis, the lipids were extracted with 2:1 chloroform:methanol (*19*) and analyzed by thin-layer chromatography (TLC) using hexane:ether:acetic acid (70:30:1) or chloroform:methanol:water:acidic acid (65:25:4:1) to separate neutral and polar lipids, respectively. Lipids were also quantified by colorimetric methods (*20*−*23*).

For density measurements, the density of the bottom fraction was adjusted to 1.25 g/mL with solid KBr, overlaid with 1.068 g/mL KBr solution, and spun in an SW60 rotor at 52 000 rpm for 22 h. Fractions were collected from the top, and their density was determined by refractometry (ABBE, Leica). Aliquots from each fraction were analyzed by negative-staining EM.

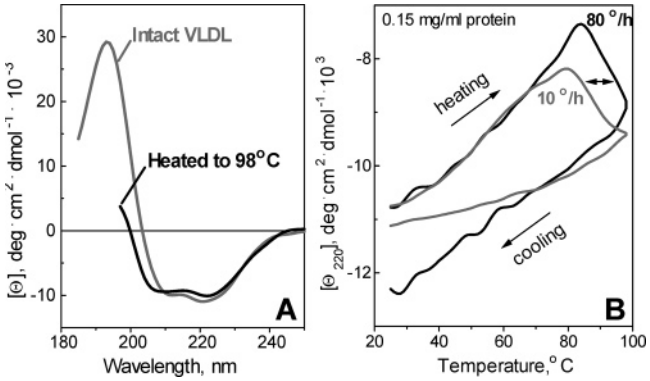

FIGURE 1: Effect of heating on the protein secondary structure in VLDL. (A) Far-UV CD spectra recorded at 25 °C of intact VLDL and of VLDL that have been heated and cooled from 25 to 98 °C at 80 °C/h. (B) CD melting curves at 220 nm recorded upon heating and cooling of VLDL at a rate of 80 °C/h (black) or 10 °C/h (gray). The data in A and B were recorded from VLDL samples of 0.15 mg/mL protein concentration in standard buffer (10 mM Na phosphate, pH 7.6).

All experiments in this study were repeated 3−8 times to ensure reproducibility.

RESULTS

To assess the effects of heating on the protein secondary structure, far-UV CD spectra were recorded from VLDL samples that were heated and cooled from 25 to 98 °C. Figure 1A shows the spectra of VLDL recorded at 25 °C before and after heating to 98 °C. The spectrum of intact VLDL is consistent with the earlier report (*12*) and indicates a mixture of α-helix and β-sheet. It partially overlaps the spectrum of heated VLDL that is cut off near 195 nm due to an irreversible heat-induced increase in turbidity (described below). This spectral overlap suggests that the secondary structure of VLDL proteins is partially retained after heating to 98 °C.

To monitor the secondary structure as a function of temperature, CD signal at 220 nm, $\Theta_{220}(T)$, was recorded during VLDL heating and cooling at a rate of 10 or 80 °C/h. Heating to less than 80 °C leads to a gradual reduction in the CD amplitude that is reversible upon cooling, as evident from the close superimposition of the heating and cooling curves (not shown); similar changes in far-UV CD were observed in a limited temperature range in plasma HDL and LDL and were attributed to secondary structural relaxation rather than global protein unfolding (*11*, *15*). VLDL heating to higher temperatures leads to a small but significant increase in the negative CD above 80 °C (Figure 1B, upper lines). This CD change may not reflect secondary structure unfolding (which leads to a reduction rather than an increase in the Θ_{220} amplitude) and may result, at least in part, from a shoulder of a large negative CD peak at 320 nm that is observed in VLDL at these temperatures and is described below. This high-temperature transition is irreversible, as indicated by non-coincident heating and cooling data in Figure 1. Furthermore, the onset of this transition shifts to lower temperatures at slower scan rates (Figure 1, double arrow). Such a scan rate effect is a hallmark of a kinetically controlled reaction with high activation energy (*23*) that is typical of lipoprotein denaturation (*9*−*11*).

To elucidate the origin of this high-temperature transition, near-UV/visible CD spectra of VLDL were recorded at 25 °C before and after heating to 98 °C. In contrast to intact VLDL, the spectrum of heated VLDL shows a large negative CD peak centered at 320 nm (Figure 2A). A similar irreversible heat-induced change in near-UV/visible CD was observed in LDL and was attributed to repacking of apolar lipids upon lipoprotein rupture and release of the apolar core (*11*). In fact, protein contribution to CD may be large only at $\lambda < 300$ nm; therefore, the CD peak at 320 nm is probably dominated by the contribution from apolar lipids such as carotenoids, TG, and CE, which are the only VLDL moieties that exhibit large induced CD at these wavelengths (*25*−*28*). Thus, the large irreversible heat-induced changes in near-UV/visible CD of VLDL suggest repacking of apolar lipids due to lipoprotein rupture.

To test this hypothesis, we correlated the heat-induced changes in near-UV/visible CD (that report on lipid repacking) and turbidity (that report on changes in the particle size and refractive index). To do so, we measured dynode voltage, *V*, in CD experiments as described (*9*, *18*). The melting data $\Theta_{320}(T)$ and $V_{320}(T)$ in Figure 2B,C were recorded simultaneously at 320 nm during VLDL heating and cooling at a rate of 10 to 80 °C/h. The heating curves in Figure 2B show a large cooperative increase in the negative CD signal; heating to higher temperatures leads to a small reduction in this negative CD that is due to lipid phase separation. Importantly, the large increase in the CD amplitude is accompanied by a large sigmoidal increase in turbidity (Figure 2C), suggesting that lipid repacking is accompanied by an increase in the particle size. Closer inspection of the heating curves in Figure 2B,C shows that the increase in turbidity precedes the CD changes by about 5 °C, suggesting that the increase in the particle size precedes repacking of apolar lipids; this may be due to VLDL fusion preceding particle rupture. Both CD and turbidity changes are irreversible, as indicated by non-coincident heating and cooling data in Figure 2B,C. Moreover, both CD and turbidity heating curves shift to lower temperature by about 6 °C upon reduction in the scan rate from 80 to 10 °C/h (Figure 2B, C), indicating high activation energy of the transition (*9*, *24*). Taken together, these results demonstrate that VLDL heating above 80 °C leads to an irreversible kinetically controlled transition that involves formation of larger particles (indicated by turbidity) followed by repacking of apolar lipids (indicated by CD at 320 nm).

Formation of larger particles upon heating must be a high-order reaction. To test the concentration dependence of this reaction, we recorded CD and turbidity melting data from VLDL samples of various concentrations under otherwise identical conditions. Turbidity heating data $V_{320}(T)$ in Figure 2D, which were recorded at a rate of 80 °C/h from VLDL solutions of 0.11−0.56 mg/mL protein concentration, show that increase in VLDL concentration leads to an increased amplitude and apparent cooperativity of the transition but has no large effect on its onset temperature.

To assess the kinetics of VLDL denaturation, we monitored the time course of the turbidity changes in T-jumps from 25 °C to higher temperatures (75−95 °C). Figure 3A shows $V_{220}(t)$ data recorded from VLDL solutions of 0.15 mg/mL protein concentration. Data fitting by double exponentials (solid lines in Figure 3A) suggests two distinct denaturation phases. The Arrhenius plots for these two phases are linear and have similar slopes that correspond to the

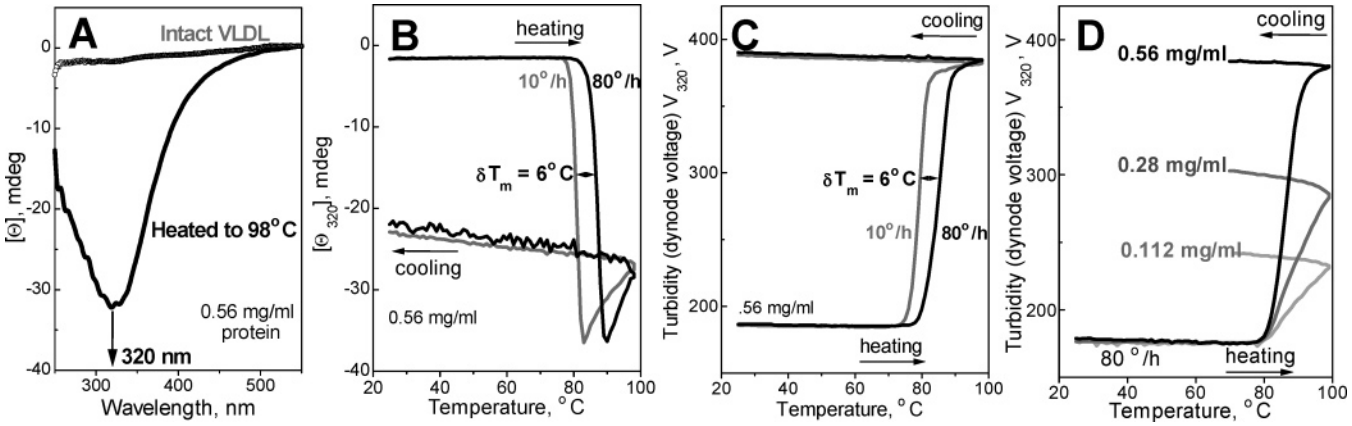

FIGURE 2: Thermal transition in VLDL monitored by near-UV/visible CD and turbidity. (A) CD spectra recorded at 25 °C of intact VLDL and of VLDL that have been heated and cooled from 25 to 98 °C at 80 °C/h rate. (B,C) Melting data $\Theta_{320}(T)$ and $V_{320}(T)$ recorded at 320 nm by CD and turbidity at a scan rate of 80 °C/h (black) or 10 °C /h (gray). (D) CD melting data recorded at 320 nm, 80 °C/h scan rate, from VLDL samples of varying protein concentrations (indicated on the lines). Cell path length in A−D is 5 mm.

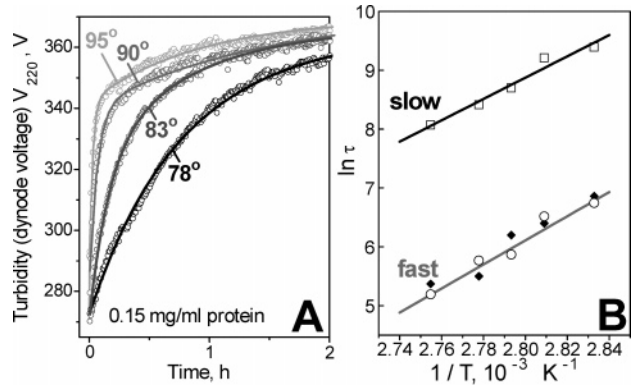

FIGURE 3: Kinetic analysis of VLDL heat denaturation. (A) Time course of thermal denaturation monitored by turbidity at 220 nm, $V_{220}(t)$, in temperature jumps from 25 °C to higher temperatures (indicated on the lines). VLDL protein concentration is 0.15 mg/mL. Data fitting by double exponentials (solid lines) suggests two kinetic phases. (B) Arrhenius analysis of the $V_{220}(t)$ data in panel A (open symbols). The Arrhenius plots for the two kinetic phases have similar slopes that correspond to activation energy $E_a = 53 \pm 7$ kcal/mol. At higher VLDL concentrations (0.56 mg/mL protein), $V_{220}(t)$ data are well-approximated by monoexponentials corresponding to the fast kinetic phase (solid symbols).

activation energy $E_a = 53 \pm 7$ kcal/mol (Figure 3B). The error in this estimate incorporates the fitting errors and the discrepancies among the data sets recorded from different VLDL pools.

Similar T-jump data recorded from samples of higher VLDL concentration (0.5−0.6 mg/mL protein, data not shown) are well-approximated by single exponentials that correspond to the faster kinetic phase, as illustrated by the overlapping Arrhenius plots (Figure 3B, closed and open symbols). Thus, increasing VLDL concentration causes no large changes in the Arrhenius activation energy E_a but accelerates the slow phase, resulting in a single-phase reaction.

The two-exponential denaturation kinetics observed at low VLDL concentrations may reflect sample heterogeneity or distinct reaction steps. The former is unlikely, since the highly heterogeneous total VLDL pool shows similar two-phase kinetics to the more homogeneous $VLDL_2$ subclass isolated from this pool. Alternatively, the two-exponential kinetics may reflect two phases corresponding to distinct morphologic transitions in VLDL. To identify these transitions, we used negative staining EM to visualize the particles at various stages of thermal denaturation.

In one series of experiments, a VLDL sample of 0.15 mg/mL protein concentration was heated at a constant rate of 80 °C/h and the aliquots taken at several temperatures from the transition range were analyzed by EM (Figure 2B,C). Figure 4A shows intact particles ranging in diameter from 40 to 60 nm, which is typical of human $VLDL_2$. Figure 4B shows that heating to 83 °C leads to an increase in the particle size that is consistent with the increased turbidity (Figure 2C) and occurs via two mechanisms. First, round-shaped lipoprotein-like particles of larger diameters are observed that are apparent products of VLDL fusion; also, clusters of aggregated particles are seen that contain intact-size and fused VLDL along with occasional lipid droplets that may be formed by coalescence of apolar core lipids released from ruptured VLDL (Figure 4B). Similarly, heat- or denaturant-induced lipoprotein fusion and rupture were observed in plasma HDL and LDL (*10*, *11*, *15*). Figure 4C shows that heating to 90 °C leads to conversion of all VLDL-like particles into large lipid droplets, suggesting extensive rupture; these results are in good agreement with the CD and turbidity heating curves in Figure 2B,C and show that VLDL fusion (which leads to the initial increase in the particle size observed by turbidity) is followed by VLDL rupture and repacking of apolar lipids (observed by CD). Remarkably, small round-shaped particles are also formed at 90 °C (Figure 4C). The diameters of these particles range from 8 to 13 nm (which is similar to plasma HDL), with an average diameter $\langle d \rangle = 10-12$ nm observed for lipoproteins from different plasma pools (Figure 4E). Formation of such HDL-size particles has never before been reported in the lipoprotein denaturation studies. Finally, heating to 98 °C, i.e., to the completion of the CD and turbidity transition (black lines in Figure 2B,C), leads to a complete conversion of all lipoprotein-like particles into lipid droplets and to the appearance of thin density streaks (Figure 4D) whose size and morphology are consistent with dissociated apoB (*29*); similar density streaks have been observed at the final stage of thermal disruption of LDL (*11*). Thus, similar to HDL and LDL, VLDL heating leads to lipoprotein fusion, rupture, and protein dissociation. In addition, transient

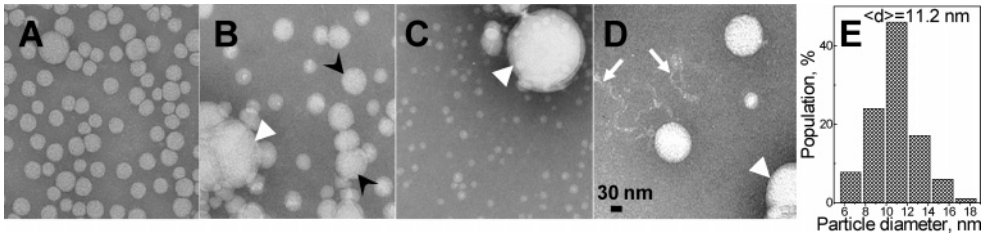

FIGURE 4: Heat-induced morphological transitions in VLDL monitored by negative-staining electron microscopy. A VLDL sample of 0.15 mg/mL protein concentration was heated at 80 °C/h; sample aliquots were taken at several temperatures from the transition range and were visualized by EM. Intact VLDL (A) and VLDL heated to 83 °C (B), 87 °C (C), and 98 °C (D) are shown. (E) Size histogram for the small particles observed in panel C. Fused VLDL (black arrowheads), lipid droplets (white arrowheads), and density streaks consistent with dissociated apoB (white arrows) are indicated.

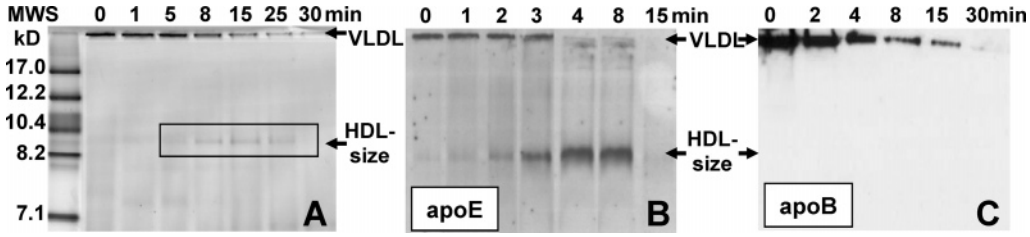

FIGURE 5: Time course of thermal disruption of VLDL monitored by nondenaturing PAGE and Western blotting. VLDL samples of 0.56 mg/mL protein concentration were incubated at 83 °C for 120 min. Sample aliquots were taken after different incubation times (indicated on the lanes in min); 0 indicates intact VLDL. Incubation for over 30 min led to no additional changes in the data (not shown). Nondenaturing PAGE stained with Coomassie blue (A) and a similar PAGE followed by immunoblotting using antibodies for apoE (B) or apoB (C) are shown. The bands corresponding to intact VLDL and to HDL-size particles are indicated. Single-donor VLDL from donor A were used to record the data in panel A, and from donor B to record the data in panels B and C; these VLDL showed different relaxation times for the first kinetic phase during which HDL-size particles are formed ($\tau_1 = 15$ min for donor A and 8 min for donor B), which explains slower reaction time course in panel A as compared to panels B and C.

dissociation of small HDL-size particles is observed that is unique to VLDL (Figure 4C).

In another series of experiments, a VLDL sample of 0.15 mg/mL protein concentration was subjected to a T-jump to 83 °C; sample aliquots were taken after incubation at 83 °C for up to 120 min and were visualized by negative-staining EM. Incubation for 3 min led to extensive fusion and partial aggregation of VLDL, similar to that observed in Figure 4B. Incubation for 10 min (which corresponds to the exponential relaxation time τ_{fast} for the fast kinetic phase determined from the T-jump turbidity data) resulted in extensive VLDL rupture and dissociation of small HDL-size particles, similar to those in Figure 4C. Incubation for 120 min (which corresponds to the exponential relaxation time τ_{slow} for the slow kinetic phase) leads to coalescence of all lipoprotein-like particles into large lipid droplets and to formation of density streaks that are consistent with dissociated apoB, similar to those seen in Figure 4D. Thus, the correlation of the EM and turbidity data suggests that the faster kinetic phase in VLDL denaturation involves VLDL fusion, partial rupture, and release of small HDL-size particles, while the slower phase involves complete lipoprotein disintegration and lipid coalescence into large droplets, along with apparent dissociation of apoB.

To further analyze the nature of the transiently occurring HDL-size particles, VLDL samples of 0.5−0.6 mg/mL protein concentration were subjected to a T-jump to 83 °C and the aliquots taken during the first hour of incubation at 83 °C were analyzed by nondenaturing PAGE. At high sample concentrations used in these experiments, VLDL denaturation shows only one relatively fast kinetic phase (Figure 3B) with relaxation time $\tau_1 = 5-10$ min for VLDL from different plasma pools. Nondenaturing PAGE shows that the band corresponding to intact VLDL gradually disappears during the first 30 min of incubation (Figure 5A), which is consistent with VLDL fusion, aggregation, and rupture observed by EM at this temperature (Figure 4B). In addition, formation of small HDL-size particles ($d \sim 9$ nm) is observed after 5−25 min incubation (which encompasses $\tau_{fast} = 10$ min for this sample); this result is consistent with the average size of the small particles determined by EM (Figure 4C). After prolonged incubation (30 min or more), the band corresponding to these small particles disappears (Figure 5A), which is consistent with disappearance of HDL-size particles observed by EM upon prolonged incubation at 83 °C or gradual heating above 90 °C (Figure 4D). Taken together, our kinetic studies by turbidity, EM, and nondenaturing PAGE indicate that the transient formation of HDL-size particles occurs during the fast kinetic phase of VLDL denaturation.

The protein composition of the total products of VLDL denaturation was assessed as follows. VLDL at various stages of thermal denaturation at 83 °C were subjected to nondenaturing PAGE followed by immunoblotting using antibodies to apoE and apoB. The results in Figure 5B,C clearly show that, in contrast to intact VLDL that contain both exchangeable (apoE) and nonexchangeable proteins (apoB), the small particles dissociated from VLDL contain apoE but no apoB.

Protein composition of the HDL-size particles was also analyzed by SDS PAGE. VLDL were incubated for up to 15 min at 83 °C to maximize the population of the small particles, followed by centrifugation at 13 000 rpm for 20−30 min. The bottom fraction contained mainly HDL-size particles with trace amounts of fused VLDL (as indicated by EM, data not shown); this fraction was used for the biochemical analysis. SDS PAGE analysis of this fraction shows that it contains apoE and apoCs but no apoB (Figure

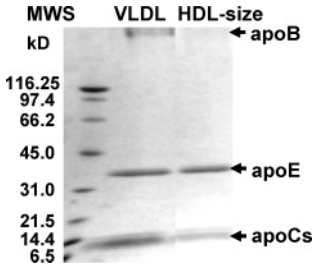

FIGURE 6: Protein composition of intact VLDL and of the small HDL-size particles transiently formed during VLDL heating. The particles were obtained by VLDL incubation at 83 °C for 15 min followed by cooling to 22 °C and centrifugation at 13 000 rpm for 30 min. SDS PAGE of these particles and of intact VLDL is shown. The bands corresponding to the major VLDL proteins (apoB, apoE, and apoCs) are indicated.

6). Thus, the data in Figures 5 and 6 consistently show that, similar to HDL but in contrast to intact VLDL, the small particles dissociated from VLDL contain only exchangeable proteins (apoE and possibly apoCs) but no apoB.

Lipid composition of the bottom fraction was assessed by TLC and by enzymatic assays. The results showed polar (phospholipids, unesterified cholesterol) and apolar lipids (CE and TG) but no lyso-phospholipids (and hence no lipolysis). Consequently, the HDL-size particles contain polar surface and apolar core and thereby resemble spherical lipoproteins. Spherical shape is also consistent with exclusively round-shape appearance of the HDL-size particles observed by negative staining EM (Figure 4C).

Importantly, density gradient centrifugation followed by EM analysis of individual fractions showed the presence of exclusively HDL-size particles in the density range from 1.109 to 1.186 g/mL, which is similar to the density of plasma HDL. Low particle yield precluded accurate lipid and protein quantification in these density fractions.

In summary, the small particles dissociated from VLDL resemble mature plasma HDL in their spherical shape, size, and density and the presence of only exchangeable proteins on their surface.

DISCUSSION

The results reported here confirm that the kinetic mechanism provides a universal natural strategy for lipoprotein stabilization. They demonstrate that, similar to HDL and LDL, VLDL are stabilized by free energy barriers that decelerate morphologic lipoprotein transitions such as fusion and rupture. In fact, turbidity data in Figure 3A show that, in a near-neutral low-salt solution at 78−95 °C, these VLDL transitions occur on a time scale of hours to minutes. Linear extrapolation of the Arrhenius plots in Figure 3B to 37 °C suggests that, at near-physiologic temperatures, spontaneous VLDL fusion and rupture occur on a time scale of years, much longer than the lipoprotein lifetime in plasma (days). Although the rates of lipoprotein transitions may be affected by solvent ionic conditions (*15*) and other plasma factors, it is clear that spontaneous remodeling and fusion of VLDL under physiologic conditions is extremely slow and thus is subject to enzymatic control.

Interestingly, heating induces not only fusion and rupture of VLDL but also transient dissociation of HDL-size particles. Similar to mature HDL, these particles have an apolar core of CE and TG and polar surface composed of phospholipids and exchangeable apolipoproteins. In contrast to HDL, these particles contain apoE and possibly apoCs but no apoA-I. This may explain relatively low stability of these small particles that disappear (apparently due to rupture) upon fast heating beyond 90 °C or prolonged incubation at 83 °C (Figure 4D); in contrast, plasma HDL are highly thermostable and remain intact under these conditions (*15*). Thus, the small particles dissociated from VLDL upon heating are similar to mature HDL in size, density, and spherical morphology but are different in their protein composition and stability.

We propose that the HDL-like particles dissociated from VLDL may mimic aspects of apoE transfer between TG-rich lipoproteins and HDL in plasma. The key steps in the metabolism of TG-rich lipoproteins include VLDL conversion to IDL by lipoprotein lipase followed by IDL to LDL conversion by hepatic lipase. In these reactions, the particle core shrinks due to TG lipolysis and the excess surface components (exchangeable apolipoproteins and polar lipids) transfer to HDL (refs *30* and *31* and references therein). Transfer of apoE from TG-rich lipoproteins to HDL in the fasted state occurs via the lipid-bound protein form that resembles discoidal or spherical HDL and contributes to the significant fraction of plasma HDL (∼10%) that contain apoE but no apoA-I (ref *32* and references therein). In plasma, apoE facilitates CE core expansion in HDL upon CE accumulation and thereby plays an important role in HDL metabolism, particularly in case of cholesterol ester transfer protein deficiency (*33*, *34*). Thus, apoE-containing HDL, which may be generated during lipolysis of TG-rich proteins, are important players in lipoprotein metabolism.

ApoE-containing plasma HDL, which belong to HDL_2 subclass ($d = 9-17$ nm) (*34*, *35*), are similar in size to apoE-containing HDL-like particles observed in this work (Figure 4C,E; Figure 5). Formation of these small particles follows heat-induced VLDL fusion (Figure 4B,C) and thereby provides a mechanism for removing excess surface components from the fused particles. Thus, different modes of VLDL perturbation (such as lipase-mediated TG hydrolysis or heat-induced VLDL fusion) may lead to transient formation of similar apoE-containing HDL-like particles.

Earlier studies of HDL and LDL have shown that thermal and solute-induced perturbations may mimic aspects of enzymatic lipoprotein remodeling such as particle fusion, apolipoprotein dissociation, and phospholipid transfer (*10*, *11*, *36*, *37*). The results reported here extend this notion to VLDL and suggest that thermal perturbation of VLDL mimics aspects of protein and lipid transfer among TG-rich lipoproteins and HDL pools in plasma.

ACKNOWLEDGMENT

We are indebted to Michael Gigliotti for help with biochemical assays, to Donald L. Gantz for help with electron microscopy, to Dr. Shobini Jayaraman and Sangeeta Benjwal for experimental help, and to Dr. David Atkinson for invaluable advice.

REFERENCES

1. Anber, V., Millar, J. S., McConnell, M., Shepherd, J., and Packard, C. J. (1997) Interaction of very-low-density, intermediate-density, and low-density lipoproteins with human arterial wall proteoglycans, *Arterioscler. Thromb. Vasc. Biol. 17* (11), 2507−2514.

2. Demant, T., and Packard, C. (1998) In vivo studies of VLDL metabolism and LDL heterogeneity, *Eur. Heart J. 19* (Suppl. H), 7−10.
3. Krauss, R. M. (1998) Atherogenicity of triglyceride-rich lipoproteins, *Am. J. Cardiol. 81* (4A), 13B−17B.
4. Shelness, G. S., and Sellers, J. A. (2001) Very-low-density lipoprotein assembly and secretion, *Curr. Opin. Lipidol. 12* (2), 151−157.
5. Skalen, K., Gustafsson, M., Rydberg, E. K., Hulten, L. M., Wiklund, O., Innerarity, T. L., and Boren, J. (2002) Subendothelial retention of atherogenic lipoproteins in early atherosclerosis, *Nature 417*, 750−754.
6. Segrest, J. P. (2002) The role of non-LDL:non-HDL particles in atherosclerosis, *Curr. Diabetes Rep. 2* (3), 282−288.
7. Olofsson, S. O., and Boren, J. (2005) Apolipoprotein B: a clinically important apolipoprotein which assembles atherogenic lipoproteins and promotes the development of atherosclerosis, *J. Intern. Med. 258* (5), 395−410.
8. Segrest, J. P., Jones, M. K., De Loof, H., and Dashti, N. (2001) Structure of apolipoprotein B-100 in low density lipoproteins, *J. Lipid Res. 42* (9), 1346−1367.
9. Gursky, O., Ranjana, R., and Gantz, D. L. (2002) Complex of human apolipoprotein C-1 with phospholipid: Thermodynamic or kinetic stability?, *Biochemistry 41*, 7373−7384.
10. Mehta, R., Gantz, D. L., and Gursky, O. (2003) Human plasma high-density lipoproteins are stabilized by kinetic factors, *J. Mol. Biol. 328* (1), 183−192.
11. Jayaraman, S., Gantz, D. L., and Gursky, O. (2005) Structural basis for thermal stability of human low-density lipoprotein, *Biochemistry 44* (10), 3965−3971.
12. Chen, G. C., and Kane, J. P. (1979) Secondary structure in very low density and intermediate density lipoproteins of human serum, *J. Lipid Res. 20* (4), 481−488.
13. Parks, J. S., Atkinson, D., Small, D. M., and Rudel, L. L. (1981) Physical characterization of lymph chylomicra and very low density lipoproteins from nonhuman primates fed saturated dietary fat, *J. Biol. Chem. 256*, 12992−12999.
14. Hale, J. E., and Schroeder, F. (1981) Differential scanning calorimetry and fluorescence probe investigations of very low density lipoprotein from the isolated perfused rat liver, *J. Lipid Res. 22*, 838−851.
15. Jayaraman, S., Gantz, D. L., and Gursky, O. (2006) Effects of salt on thermal stability of human plasma high-density lipoproteins, *Biochemistry 45*, 4620−4628.
16. Schumaker, V. N., and Puppione, D. L. (1986) Sequential flotation ultracentrifugation, *Methods Enzymol. 128*, 155−170.
17. Markwell, M. A., Haas, S. M., Bieber, L. L., and Tolbert, N. E. (1978) A modification of the Lowry procedure to simplify protein determination in membrane and lipoprotein samples, *Anal. Biochem. 87* (1), 206−210.
18. Benjwal, S., Verma, S., Röhm, K. H., and Gursky, O. (2006) Monitoring protein aggregation during thermal unfolding in circular dichroism experiments, *Protein Sci. 15*, 635−639.
19. Folch, J., Lees, M., and Sloane Stanley, G. H. (1957) A simple method for the isolation and purification of total lipids from animal tissues, *J. Biol. Chem. 226* (1), 497−509.
20. Bartlett, G. R. (1959) Phosphorus assay in column chromatography, *J. Biol. Chem. 234* (3), 466−468.
21. Tercyak, A. M. (1991) Determination of cholesterol and cholesterol esters, *J. Nutr. Biochem. 2*, 281−292.
22. Fossati, P., and Prencipe, L. (1982) Serum triglycerides determined colorimetrically with an enzyme that produces hydrogen peroxide, *Clin. Chem. 28*, 2077−2080.
23. McGowan, M. W., Artiss, J. D., Strandbergh, D. R., and Zak, B. (1983) A peroxidase-coupled method for the colorimetric determination of serum triglycerides, *Clin. Chem. 29*, 538−542.
24. Sanchez-Ruiz, J. M. (1992) Theoretical analysis of Lumry-Eyring model in differential scanning calorimetry, *Biophys. J. 61*, 921−935.
25. Chen, G. C., and Kane, J. P. (1974) Contribution of carotenoids to the optical activity of human serum low-density lipoprotein, *Biochemistry 13* (6), 4706−4712.
26. Sklar, L. A., Craig, I. F., and Pownall, H. J. (1981) Induced circular dichroism of incorporated fluorescent cholesteryl esters and polar lipids as a probe of human serum low density lipoprotein structure and melting, *J. Biol. Chem. 256* (9), 4286−4292.
27. Yeagle, P. L., Bensen, J., Greco, M., and Arena, C. (1982) Cholesterol behavior in human serum lipoproteins, *Biochemistry 21* (6), 1249−1254.
28. Chen, G. C., Chapman, M. J., and Kane, J. P. (1983) Secondary structure and thermal behavior of trypsin-treated low-density lipoproteins from human serum, studied by circular dichroism, *Biochim. Biophys. Acta 754* (1), 51−56.
29. Gantz, D. L., Walsh, M. T., and Small, D. M. (2000) Morphology of sodium deoxycholate-solubilized apolipoprotein B-100 using negative stain and vitreous ice electron microscopy, *J. Lipid Res. 41* (9), 1464−1472.
30. Musliner, T. A., Long, M. D., Forte, T. M., Nichols, A. V., Gong, E. L., Blanche, P. J., and Krauss, R. M. (1991) Dissociation of high density lipoprotein precursors from apolipoprotein B-containing lipoproteins in the presence of unesterified fatty acids and a source of apolipoprotein A-I, *J. Lipid Res. 32* (6), 917−933.
31. Chung, B. H., Tallis, G.,Yalamoori, V., Anantharamaiah, G. M., and Segrest, J. P. (1994) Liposome-like particles isolated from human atherosclerotic plaques are structurally and compositionally similar to surface remnants of triglyceride-rich lipoproteins, *Arterioscler. Thromb. 14* (*4*), 622−635.
32. Rye, K. A., Bright, R., Psaltis, M., and Barter, P. J. (2006) Regulation of reconstituted high density lipoprotein structure and remodeling by apolipoprotein E, *J. Lipid Res. 47* (5), 1025−1036.
33. Matsuura, F., Wang, N., Chen, W., Jiang, X. C., and Tall, A. R (2006) HDL from CETP-deficient subjects shows enhanced ability to promote cholesterol efflux from macrophages in an apoE- and ABCG1-dependent pathway, *J. Clin. Invest. 116* (5), 1435−1442.
34. Krimbou, L., Marcil, M., Chiba, H., and Genest, J., Jr. (2003) Structural and functional properties of human plasma high density-sized lipoprotein containing only apoE particles, *J. Lipid Res. 44* (5), 884−892.
35. Mahley, R. W., Huang, Y., and Weisgraber, K. H. (2006) Putting cholesterol in its place: apoE and reverse cholesterol transport, *J. Clin. Invest. 116* (5), 1226−1229.
36. Jayaraman, S., Gantz, D. L., and Gursky, O. (2004) Polyethylene glycol induces fusion and destabilization of human plasma high-density lipoproteins, *Biochemistry 43* (18), 5520−5531.
37. Pownall, H. J. (2006) Detergent-mediated phospholipidation of plasma lipoproteins increases HDL cholesterophilicity and cholesterol efflux via SR-BI, *Biochemistry 45* (38), 11514−11522.

BI7001532